

Simulating evapotranspiration and photosynthesis of winter wheat over the growing season

Xingguo Mo*, Suxia Liu¹

Institute of Geographic Sciences and Natural Resources Research, Chinese Academy of Sciences, Beijing 100101, PR China

Received 6 September 1999; received in revised form 28 May 2001; accepted 28 May 2001

Abstract

A soil–vegetation–atmosphere process model is established to simulate water, energy and CO₂ fluxes. The model includes: (1) an improved multi-layer canopy radiative transfer submodel; (2) a new canopy conductance/photosynthesis submodel that distinguishes sunlit and shaded leaves; (3) a two-source soil–canopy energy balance submodel; (4) a multi-layer soil water and heat transfer submodel. The model is validated using two groups of data collected in a winter wheat field transitioning from recovering green through to maturity (in 1992) and from overwintering to maturity (in 1998) at Yucheng Experimental Station, Chinese Academy of Sciences in North China Plain. Satisfactory agreement is obtained between simulated and measured energy partitioning, surface temperature, root zone soil moisture, and canopy photosynthesis. Model-derived rates of daily crop transpiration and soil evaporation are in agreement with field measurements obtained via lysimeter and the Bowen ratio method. Sensitivity results show that the Leuning model of stomatal conductance/photosynthesis gives better evapotranspiration estimates than the Jarvis and Ball–Berry models. There are significant differences between the photosynthesis rates produced from our model and the corresponding rates calculated by the traditional “big leaf” model, which does not differentiate sunlit and shaded effects. However, both models generate fairly similar evapotranspiration rates. The successful simulation in 1998 was achieved using meteorological station data alone as driving force of the model instead of using micrometeorological data as in 1992 case, suggesting that the new model could have general applicability without the need for detailed micrometeorological data. © 2001 Elsevier Science B.V. All rights reserved.

Keywords: Simulation; Model; Winter wheat; Evapotranspiration; Photosynthesis

1. Introduction

Estimating evapotranspiration and photosynthesis from meteorological data is important for crop growth monitoring, irrigation scheduling, and water resources

management in general. A standard approach to obtain such estimates is through the application of soil–vegetation–atmosphere transfer (SVAT) models. The SVAT “big-leaf” models have been shown to be inadequate in this regard because of the errors introduced by treating the canopy and underlying substrate as a single source (Acs, 1994). A better approximation to reality can be achieved by the two-source SVAT models, which differentiate the canopy and the substrate. Such models incorporate soil and vegetation physical processes as well as interactions between soil, vegetation and atmosphere (Shuttleworth

* Corresponding author Fax: +86-10-64889684.

E-mail addresses: moxg@igsnr.ac.cn (X. Mo),
suxia@maths.unsw.edu.au (S. Liu).

¹ Present address: School of Mathematics, The University of New South Wales, Sydney, NSW 2052, Australia. Fax: +61-2-9385-7123.

and Wallace, 1985; Choudhury and Monteith, 1988; Mihailovic and Ruml, 1996; Wang and Leuning, 1998). In a two-source model, the canopy component is treated either as a single big leaf, or as partitioned shaded-sunlit leaves (Sellers et al., 1996; Tourula and Heikiheimo, 1998; Boegh et al., 1999). Transports of heat and soil moisture are often represented with three or more layers (Flerchinger et al., 1998). Based on the advances in biochemistry of photosynthesis and physiology of stomatal behavior, a coupled stomatal conductance/photosynthesis model (Ball et al., 1987; Collatz et al., 1991) has been incorporated successfully in both multi-layer (Leuning et al., 1995; Sellers et al., 1996; Su et al., 1996; Wang and Leuning, 1998) and big leaf (Amthor, 1994) SVAT models.

In nature leaf photosynthesis rates respond non-linearly to the absorbed photosynthetically active radiation (PAR), and canopy leaves experience a wide range of irradiance densities. It is not surprising, therefore, that traditional big leaf photosynthesis models may generate errors up to 45% when utilizing only absorbed radiation by leaves (Myneni and Ganapol, 1992). In order to obtain a more reliable simulation of photosynthesis, it is necessary to incorporate the irradiance of sunlit and shaded leaves in more detail in the canopy radiative transfer model.

The object of this paper is to present a new soil–vegetation–atmosphere process model for investigating evapotranspiration and photosynthesis in C_3 crops. The model includes improved submodels for both multi-layer canopy radiation and photosynthesis–stomatal conductance. Assimilation rates for sunlit and shaded leaves are obtained separately using the fraction of leaf area index and the absorbed PAR for each type of leaf. Profiles of air temperature, humidity and CO_2 are treated as uniform as these factors are less important as photosynthesis constraints.

In our radiation submodel, to better approximate reality we replace single leaf reflectivity and transmissivity with upward and downward scattering coefficients for each subdivided canopy layer. A bare soil surface is assumed in the soil water and heat transfer submodel. Soil moisture and heat flow transport is simulated with a multi-layer representation scheme, which models the soil moisture distribution as a function of root density and vertical water movement.

The model was validated with field measurements from a winter wheat field over two growing seasons, using evapotranspiration estimates from a weighing lysimeter and surface energy fluxes from the Bowen ratio method. The sensitivities of evapotranspiration and/or photosynthesis rates to various formulations of stomatal conductance are investigated. A measure of the degree of the improvement from the new model is obtained by comparison with a traditional single layer model (Sellers et al., 1996).

2. Model description

The model is based on radiation, water, heat and CO_2 transfer processes over a relative uniform field plot. Fig. 1 represents the components of radiation, energy balance and resistances of the model. The detail of the model is outlined below.

2.1. One-dimensional multi-layer canopy radiation model

Because the incident radiation is the major source for the surface energy balance and canopy photosynthesis, it is important to know how much of it is absorbed by the soil–canopy system and also how it is partitioned between these two components. Leaf spectral properties are quite different for near infrared radiation and visible infrared radiation (considered PAR in this paper). Also, the penetrating processes for direct and diffuse components of radiation are quite different. Our model therefore treats these various components separately. To this end, the canopy is subdivided into 20 layers with the same leaf area being assigned to each layer. The system is also used to calculate the radiation loading of the sunlit or shaded leaves.

2.1.1. Direct radiation

It is assumed that the canopy is horizontally homogenous and leaf elements are randomly located in space. The direct beam radiation incident on the canopy is then

$$R_b(L) = R_{b,0} \exp(-EXT_r L) \quad (1)$$

where $R_{b,0}$ is the incident direct radiation above canopy, R_b the direct radiation at a level with leaf

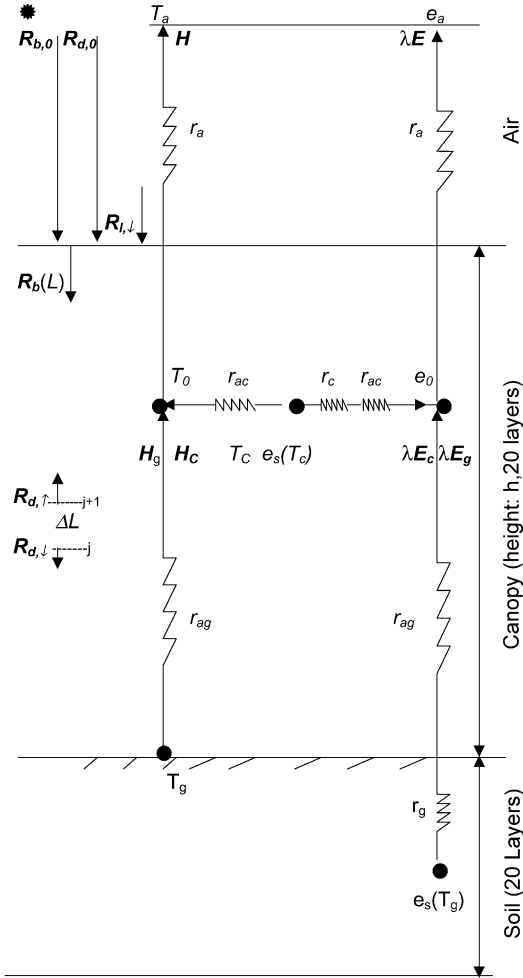


Fig. 1. The radiation components, resistances and energy balance components in the model (symbols defined in the text).

area index L , expressed on a projected area basis. The quantity EXT_r is the extinction coefficient for direct radiation, expressed as (Goudriaan, 1977):

$$EXT_r = \frac{G(\theta)(1 - \sigma_1)^{1/2}}{\cos(\theta)} \quad (2)$$

where θ is the zenith angle of solar beam, $G(\theta)$ the projection of leaves on the plane orthogonal to the incident beam and σ_1 the leaf scattering coefficient.

2.1.2. Diffuse radiation

The incident diffuse radiation is assumed to be isotropic. The fraction of diffuse radiation penetrating

without interception through each subdivided layer of the canopy is expressed as

$$I_D = 2 \int_0^{\pi/2} \exp\left(\frac{-EXT_r \Delta L}{\cos \theta}\right) \sin \theta \cos \theta d\theta \quad (3)$$

where ΔL is the leaf area index of the subdivided layer.

The upward and downward diffuse radiation is simulated with two-stream approximation equations (Norman, 1985). In Norman's model, leaf reflection and transmission coefficients are used as the scattering coefficients of the subdivided layers. This may introduce some uncertainty from a physical mechanism point of view. Rather than using leaf reflection and transmission coefficients, our model instead uses scattering coefficients of a given foliage layer ΔL for direct and diffuse components. This yields an improved version of upward and downward equations:

$$R_{d,\uparrow}^{j+1} = R_{d,\uparrow}^j [\sigma_{d,d}(1 - I_D) + I_D] + R_{d,\downarrow}^{j+1} [\sigma_{d,u}(1 - I_D)] + R_b^{j+1} \sigma_{b,u} \quad (4)$$

$$R_{d,\downarrow}^j = R_{d,\downarrow}^{j+1} [\sigma_{d,d}(1 - I_D) + I_D] + R_{d,\uparrow}^j [\sigma_{d,u}(1 - I_D)] + R_b^{j+1} \sigma_{b,d} \quad (5)$$

where j is the j th layer of canopy, and $R_{d,\uparrow}$ and $R_{d,\downarrow}$ are upward and downward diffuse radiation components, respectively. The upward and downward scattering coefficients for direct beam and diffuse radiation, denoted as $\sigma_{b,u}$, $\sigma_{b,d}$, $\sigma_{d,u}$ and $\sigma_{d,d}$, respectively, are defined in Appendix A. The solution of (4) and (5) is given by Norman (1985).

2.1.3. Longwave radiation

The transfer of longwave radiation is treated simply. The downward longwave radiation amount is calculated as (Kondo and Xu, 1997),

$$R_{l,\downarrow} = \sigma T_a^4 \left[1 - \left(1 - \frac{R_{l,\downarrow,c}}{\sigma T_a^4} \right) C \right] \quad (6)$$

while

$$C = 0.826 \left(\frac{n}{N_0} \right)^3 - 1.234 \left(\frac{n}{N_0} \right)^2 + 1.135 \frac{n}{N_0} + 0.298, \quad 0 < \frac{n}{N_0} \leq 1 \quad (7)$$

where n and N_0 are observed and possible duration of sunshine, respectively, and T_a is the air temperature at

reference height. The quantity $R_{l,\downarrow,c}$ is the downward longwave radiation amount under clear sky conditions, which is expressed as (Zuo et al., 1991):

$$R_{l,\downarrow,c} = (0.614 + 0.0557\sqrt{e_a})\sigma T_a^4 \quad (8)$$

where e_a is the air water vapor pressure (hPa) at reference height.

The longwave radiation amounts absorbed by the canopy and the soil surface beneath are calculated as (Verseghy et al., 1993):

$$R_{l,c} = (1 - \xi)(R_{l,\downarrow} + \varepsilon_g\sigma T_g^4 - 2\varepsilon_c\sigma T_c^4) \quad (9)$$

$$R_{l,g} = (1 - \xi)\varepsilon_c\sigma T_c^4 + \xi R_{l,\downarrow} - \varepsilon_g\sigma T_g^4 \quad (10)$$

where ε_c and ε_g are the emissivities of the canopy and soil, taken as 0.98 and 0.96, respectively, T_c and T_g are the temperature of canopy and soil surface, respectively, σ the Stefan–Boltzmann constant, ξ the sky view factor for soil. For most crops, it is expressed as

$$\xi = \exp(-0.8\Sigma L) \quad (11)$$

The canopy surface temperature is calculated as:

$$T_{c,s} = \frac{[(1 - \xi)\varepsilon_c T_c^4 + \xi\varepsilon_g T_g^4]^{1/4}}{\varepsilon_a} \quad (12)$$

where ε_a is the apparent emissivity of the canopy. For simplicity, it is assumed as 0.98 under both closed and sparse canopies.

2.2. Aerodynamic and soil resistances for turbulent fluxes

The stratification of wind speed and the eddy diffusion coefficient inside the canopy can be simply considered as exponential profiles:

$$u(z) = u(h) \exp\left[-\text{EXT}_w \left(1 - \frac{z}{h}\right)\right] \quad (13)$$

$$K(z) = K(h) \exp\left[-\text{EXT}_w \left(1 - \frac{z}{h}\right)\right] \quad (14)$$

where z is the height above, h the canopy height, $u(h)$ the wind speed at the canopy top and EXT_w the extinction coefficient for wind taken as 2.5. The quantity $K(h)$ is the turbulent exchange coefficient at the top of canopy, expressed as

$$K(h) = \kappa u_*(h - d) \quad (15)$$

where u_* is the friction velocity, κ the von Karman constant and d the zero displacement height.

The aerodynamic resistance for momentum and heat transfer between the canopy sink–source and the reference height is determined by surface-layer turbulence theory (Shuttleworth and Wallace, 1985):

$$r_a = \frac{1}{\kappa u_*} \ln\left(\frac{z_r - d}{h - d}\right) + \frac{h}{\text{EXT}_w K(h)} \times \left\{ \exp\left[\text{EXT}_w \left(1 - \frac{z_{o,c} + d}{h}\right)\right] - 1 \right\} \quad (16)$$

where z_r is the reference height, $z_{o,c}$ the roughness length of canopy for heat transfer, d and $z_{o,c}$ are parameterized following Shaw and Pereira (1982). The atmospheric stability correction of r_a is taken from Choudhury et al. (1986).

The aerodynamic resistance between the soil surface and canopy sink–source height is

$$r_{a,g} = \frac{h \exp(\text{EXT}_w)}{\text{EXT}_w K(h)} \left[\exp\left(-\text{EXT}_w \frac{z_{o,g}}{h}\right) - \exp\left(-\text{EXT}_w \frac{z_{o,c} + d}{h}\right) \right] \quad (17)$$

where $z_{o,g}$ is the roughness length of the soil surface for heat transfer.

Leaf boundary conductance g_1 (the reciprocal of leaf boundary resistance) depends on leaf size, shape and Reynold number (Re). Under force convection, for heat transfer, we present an expression of g_1 as (Watanabe and Mizutani, 1996):

$$g_1 = \frac{k_h}{L} (0.8 + 0.6 Re^{0.5}) \times 2 \quad (18)$$

where

$$Re = \frac{u(z)w}{\nu} \quad (19)$$

and k_h and ν are thermal molecular diffusivity and kinematic molecular diffusivity of air, respectively, and w is the characteristic dimension of an individual leaf. For the whole canopy, the integrated leaf boundary aerodynamic resistance is given by:

$$r_{a,c} = \frac{1}{\Sigma L \int_0^h g_1 dz} \quad (20)$$

Soil resistance is an empirical term describing the impedance of soil pores to the exchange of water vapor

between the soil and the immediately overlying air. We utilize the expression given by Sellers et al. (1992):

$$r_g = \exp(8.206 - 4.255W) \quad (21)$$

where W is the fraction of surface layer (0.1 m) soil moisture, expressed as a fraction of the saturated moisture content.

The total sensible heat flux (H) from the canopy (H_c) and ground (H_g) can be written as:

$$H = H_c + H_g \quad (22)$$

or

$$H = \rho_a C_p \frac{T_c - T_o}{r_{a,c}} + \rho_a C_p \frac{T_g - T_o}{r_{a,g}} \quad (23)$$

where ρ_a is the air density, C_p the specific heat of air at constant pressure and T_o the air temperature at canopy sink–source height.

H can also be expressed (Fig. 1) as

$$H = \rho_a C_p \frac{T_o - T_a}{r_a} \quad (24)$$

Similarly, the total latent heat flux can be written as

$$\lambda E = \lambda E_c + \lambda E_g \quad (25)$$

or

$$\lambda E = \lambda(E_{c,w} + E_{c,d}) + \frac{\rho_a C_p}{\gamma} \frac{e_s(T_g) - e_o}{r_{a,g} + r_g} \quad (26)$$

where λ is the latent heat of vaporization. E_c and E_g are the transpiration from canopy and evaporation from the soil surface, respectively, γ the psychrometric constant, $e_s(T_g)$ the saturated vapor pressure at the soil surface temperature and e_o the vapor pressure at canopy sink–source height. The quantity $E_{c,w}$ is the evaporation from the wetted fraction of canopy, whereas $E_{c,d}$ is the vapor flux which transpires from the dry fraction:

$$\lambda E_{c,w} = \frac{\rho_a C_p}{\gamma} \delta \frac{e_s(T_c) - e_o}{r_{a,c}} \quad (27)$$

$$\lambda E_{c,d} = \frac{\rho_a C_p}{\gamma} (1 - \delta) \frac{e_s(T_c) - e_o}{r_{a,c} + r_c} \quad (28)$$

where r_c is the canopy resistance treated in the next section. The wet fraction δ is defined as W_c/W_{cmax} , where W_c is the amount of intercepted water, W_{cmax}

the maximal possible amount of intercepted water (mm), taken as $0.2 \text{ kg m}^{-2} \Sigma L$. The quantity W_c is determined with a prognostic equation:

$$\frac{dW_c}{dt} = \xi P_r - E_{c,w} \quad (29)$$

where P_r is the rainfall and ξ is defined in Eq. (11). The daily rainfall is converted into precipitation intensity by the method of Kondo (1993).

The soil surface heat flux is obtained by

$$G = k_1 \frac{T_g - T_{s,1}}{z_{s,1}} \quad (30)$$

where k is the thermal conductivity, T_s the soil temperature and z_s the depth (positive downwards). The subscript 1 means the first depth interval below the surface.

Energy balance equations of the canopy and soil surface are

$$R_{n,c} = \lambda E_c + H_c \quad (31)$$

$$R_{n,g} = \lambda E_g + H_g + G \quad (32)$$

where $R_{n,c}$ and $R_{n,g}$ are the net radiation absorbed by the canopy and ground, respectively, calculated from the budgets of direct radiance, diffuse radiation and longwave radiation.

2.3. Stomatal conductance and photosynthesis

Stomatal behavior is an important factor for evapotranspiration simulation. Stomatal behavior is influenced by many environmental conditions and plant factors, such as radiation, the concentration of CO_2 , temperature, humidity of the air, leaf age, and soil water status. The uptake of CO_2 for photosynthesis, via stomatal conductance, can be reasonably coupled in a model of net photosynthesis (Ball et al., 1987). An important advantage is inclusion of synergistic interactions among the most important environmental stimuli.

The physiological limit of photosynthesis is primarily a function of the maximum catalytic capacity of **Ribulose-bisphosphate carboxylase-oxygenase enzyme** (Rubisco), V_m . Because V_m is linearly related to leaf nitrogen concentration which exponentially decreases in a canopy (e.g., Leuning et al., 1995), V_m should also decline exponentially with an extinction

coefficient EXT_v similar to that of diffuse radiation, expressed as

$$V_m = V_{m,o} \exp(-EXT_v L) \quad (33)$$

where $V_{m,o}$ are values of V_m at the top of canopy, taken as $200 \mu\text{mol m}^{-2} \text{s}^{-1}$, EXT_v is taken as 0.6 and L is defined in Eq. (1).

Biochemical models of photosynthesis for leaves of C_3 species have been well studied and developed (Farquhar et al., 1980). Leaf assimilation rate is limited by the efficiency of the photosynthetic enzyme system, the amount of PAR quanta captured by the leaf chlorophyll and the capacity of the leaf to transport and utilize the products of photosynthesis. The CO_2 assimilation rate A_n for C_3 leaves is expressed as (Coltatz et al., 1991):

$$A_n = \min(A_R, A_E, A_S) - R_d \quad (34)$$

where R_d is the leaf respiration rate ($\mu\text{mol m}^{-2} \text{s}^{-1}$), A_R the Rubisco limiting rate, A_E the light-limited rate, A_S the capacity for the export or utilization of the products of photosynthesis. On a leaf scale, A_R , A_E , and A_S are expressed as in Appendix B.

In our model, A_E is calculated for sunlit and shaded leaves in each subdivided layer, based on absorbed radiation and the fractions of sunlit and shaded leaf area. The fraction of sunlit leaves (f_{lt}) is given by Eq. (1).

The total assimilation rate in each sub-layer is

$$A_n = f_{lt} A_{n,lt} + (1 - f_{lt}) A_{n,sh} \quad (35)$$

where $A_{n,lt}$ and $A_{n,sh}$ are the net assimilation rates of sunlit and shaded leaves, respectively.

By integrating the assimilation rate for all layers, the entire canopy assimilation rate $A_{n,c}$ is obtained. The bulk canopy conductance (reciprocal of canopy resistance r_c) is coupled with $A_{n,c}$ and vapor pressure deficit (VPD) (Leuning et al., 1995):

$$g_c = m \frac{A_{n,c}}{(C_S - \Gamma^*)(1 + VPD_S/VPD_{S0})} + b \Sigma L \quad (36)$$

where m and b are empirical regression coefficients, taken as 11 and $0.008 \text{ mol m}^{-2} \text{s}^{-1}$, respectively. The quantity C_S is CO_2 concentration at the leaf surface, Γ^* the CO_2 compensation point, VPD_S the leaf surface VPD and VPD_{S0} is an empirical coefficient (taken as 1.5 kPa in our model).

2.4. Soil moisture and heat conduction

The transfer of heat in soil is calculated by a heat flow equation:

$$C_m \frac{\partial T_s}{\partial t} = \frac{\partial}{\partial z_s} \left(k \frac{\partial T_s}{\partial z_s} \right) \quad (37)$$

where C_m is the soil volumetric heat capacity. For estimation purpose, C_m is calculated as a weighted average of the heat capacities of soil and water (Pielke, 1984):

$$C_m = [1.2(1 - \eta_s) + 4.18\eta] \times 10^6 \quad (38)$$

The quantity k is calculated as (Camillo and Gurney, 1986):

$$k = \frac{\eta k_w + b_f(1 - \eta_s)k_s + b_a(\eta_s - \eta)k_a}{\eta + b_f(1 - \eta_s) + b_a(\eta_s - \eta)} \quad (39)$$

where k_w , k_s and k_a are water, soil solid and air thermal conductivities, respectively. b_f and b_a are weighting factors, η and η_s are, respectively, the soil volumetric water content and porosity. In our model, k_a is neglected for simplicity.

The vertical flux of soil moisture is calculated as

$$\frac{\partial \eta}{\partial t} = \frac{\partial}{\partial z_s} \left(D_w \frac{\partial \eta}{\partial z_s} - K_w \right) - S_u(z_s, t) \quad (40)$$

The soil matric potential ψ , hydraulic conductivity K_w and hydraulic diffusivity D_w are computed as (Clapp and Hornberger, 1978):

$$\psi = \psi_s \left(\frac{\eta}{\eta_s} \right)^B \quad (41)$$

$$K_w = K_{w,s} \left(\frac{\eta}{\eta_s} \right)^{2B+3} \quad (42)$$

$$D_w = K_w \frac{\partial \psi}{\partial \eta} \quad (43)$$

where ψ_s and $K_{w,s}$ are saturated soil water potential (m) and hydraulic conductivity. According to Clapp and Hornberger (1978), Eq. (41) is correct only when $\psi \geq \psi_r$ where ψ_r is matric potential at the air entry value (i.e., at a very slight suction). When $\psi < \psi_r$, there is another expression to calculate ψ , which is not given here because it did not occur in our application. The quantity B is an empirical constant set to 4.9.

The rate of root water uptake from each soil layer in the rooting zone, $S_u(z_s^i, t)$, is computed using a weighting function F_r^i , defined on the basis of the fractional volume of roots R_T and ψ in the layer (Verseghy et al., 1993):

$$S_u(z_s^i, t) = E_c \frac{F_r^i}{z_s^i - z_s^{i-1}} \quad (44)$$

and

$$F_r^i = R_T^i \frac{\psi_{cr} - \psi^i}{\sum_1 (\psi_{cr} - \psi^i)} \quad (45)$$

where i is the i th subdivided soil layer, ψ_{cr} the critical soil moisture at which transpiration ceases (in our model it is taken as -150 m), E_c is defined in Eq. (25).

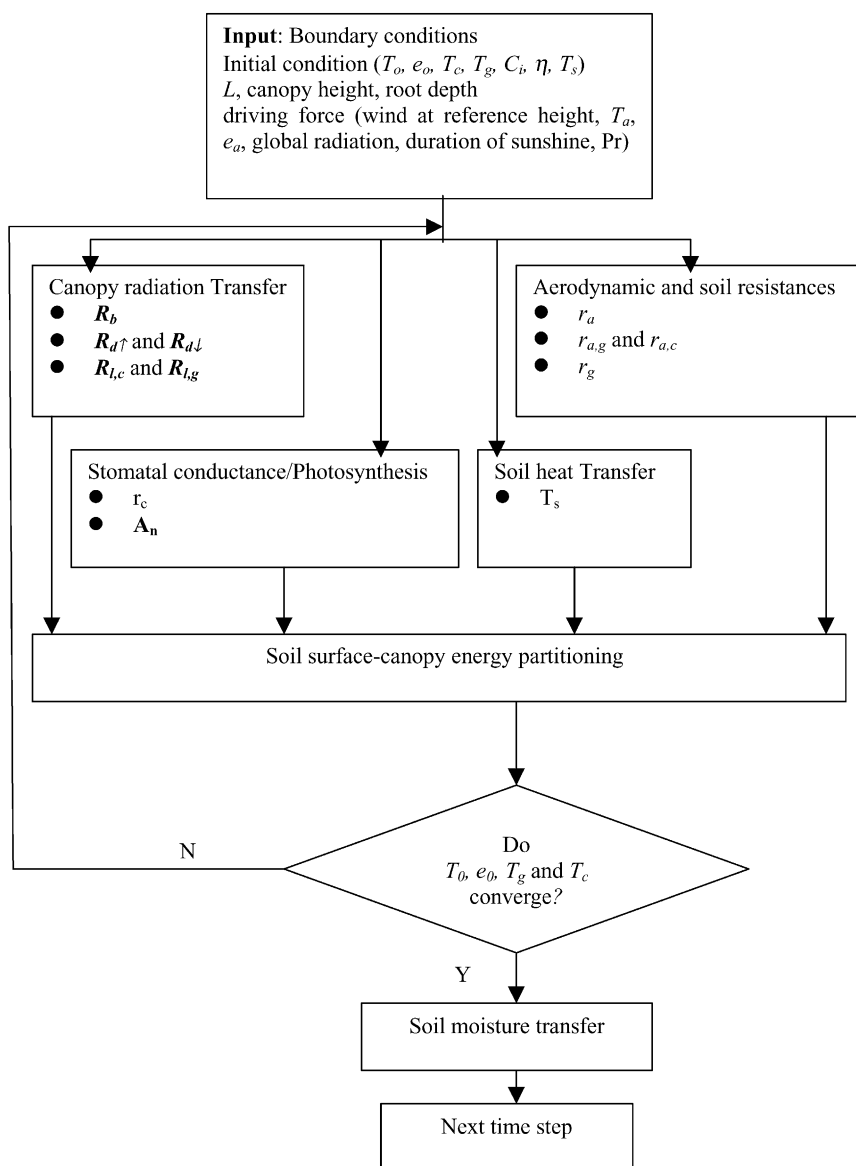


Fig. 2. Flow chart of model operation.

Eqs. (37) and (40) are discretized by finite difference method, and are solved by a Crank–Nicholson scheme. The soil is divided into 20 layers of 0.005, 0.01, 0.02, ..., 0.09, 1, 1.2, ..., 1.8 and 2 m depth. The upper boundary condition is that the moisture flux equals the infiltration or evaporation rate. The lower boundary condition is that the water flux is set as freely draining for shallow or zero for deep groundwater.

2.5. Model operation

The model was written in Fortran 77 and the model structure is shown in the flowchart in Fig. 2. An energy balance time step of 10 min was used for the application of the model to 1992 data and 60 min time step was used for the 1998 data. A 1 min time step was used for soil moisture and heat balance calculations. For the data sets used here, the speed of the calculation was about 5 min per simulation with a Pentium-350 PC. Convergence was always achieved and typically 5–30 iterations were required.

3. Experimental site, measurements, and parameters

Field measurements were carried out in a winter wheat field at Yucheng Experimental Station in March–June 1992, and January–June 1998. The

station is located 50 m above sea level in the North China Plain (37°53'N, 115°41'E). In both 1992 and 1998 the experiments covered the growth stages of recovering green, jointing, flowering, milking and maturity. Only the 1998 sampling periods experienced the overwintering stage. Soil texture of the root zone is sandy loam. Prevailing southeasterly winds were experienced during both experimental campaigns, and there was at least 1 km wind fetch available. The field was irrigated two to three times with 60–110 mm water applied each time from January to June in both years. Fig. 3 shows the information for 1998. Near the winter wheat field, a meteorological station recorded air temperature, humidity, atmospheric pressure, global radiation, wind speed and daily sunshine duration.

A 3 m mast was used for micrometeorological measurement. The measurement of wind speed, dry and wet bulb temperature was made in two subsequent levels. The upper level was 2 m above the ground, the lower level is adjusted successively as the canopy increased in height, but was normally 0.5 m above the top of the canopy. The psychrometer at each level used platinum resistance sensor units covered by ventilated plastic cylinder shields. The ventilation rate was 3 m s^{-1} . Air humidity and the Bowen ratio were calculated from the dry and wet bulb temperatures. Net radiation was measured with a net radiometer, solar irradiance with a downward-facing pyranometer and soil heat flux with two heat flux plates. The net radiometer was not heated or ventilated. Soil

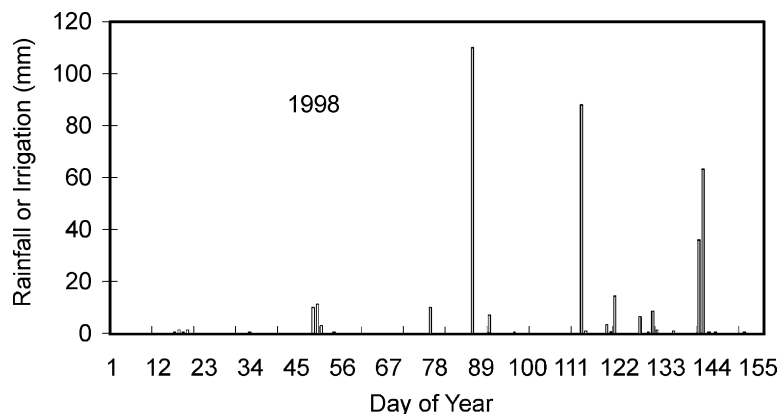


Fig. 3. The rainfall/irrigation amount over the growing season in 1998.

temperatures were measured at surface 0.05, 0.1, 0.15 and 0.2 m by thermocouples. All sensors were connected to a data logger (DataTaker, Australia). In 1992, the psychrometers were interchanged every 5 min, and the data logger scanned them every 15 s and recorded data as 5 min averages. In 1998, scanning was 5 min before and after each hour and 10 min averages were recorded.

Soil moisture was measured for every 7 days with three neutron probes near the mast. The measurements were made to a depth of 1.5 m with 0.2 m increments. At the same time soil moisture content over 0–0.5 m was also measured gravimetrically with 0.1 m increments.

The radiometric surface temperature was measured with a hand-held infrared thermometer (Matsushita Communication Industrial, Japan), tilted 45° (below horizon) and calibrated with a black body thermometer. Leaf photosynthetic rate was measured by a CO₂ analysis system (CID, USA), and five sunlit leaves were sampled each time at the canopy top. The air at 3 m high was pumped into the tube of CO₂ analysis system. For each observation, leaf photosynthesis was averaged from five upper surface measurements. Measurements were made at 8:00, 10:00, 12:00, 14:00, 16:00 and 18:00 h in March–May in 1998.

Evapotranspiration rate was also measured with a weighing lysimeter, with a circular surface area of 3.14 m² and depth of 5 m. The lysimeter was supported by a lever whose displacement is measured with a resolution of 0.02 mm water depth equivalent. A lever with 102 steel cables, fixed by pulley block, are used to suspend the mechanism. The lever has a dip angle of 0.08° so that the cables make small displacements if the lysimeter weight changes. In the lysimeter, wheat stalk density and groundwater depth were similar to the surrounding field. The lysimeter weight was recorded at 8:00 and 20:00 h each day.

Plant samples were taken every 10 days including 20–40 stalks. Leaf area was determined by measuring the width and length of each leaf. Leaf area index (*L*) was obtained by multiplying the leaf area of each stalk by plant density in the field. The total net ecosystem productivity of winter wheat was about 2 kg m⁻² and the water use efficiency (the total biomass over total ET) is about 0.008 g CO₂ (g H₂O)⁻¹ over the whole growing season in these 2 years.

4. Results

Parameters used in the model were either measured or taken from the literature. The key parameters used are shown in Table 1.

The model was run from the recovering green to maturity stage of winter wheat in 1992 and from overwintering to maturity stage in 1998. The input forcing data included air temperature, water vapor pressure, wind speed, global radiation, duration of sunshine and precipitation/irrigation amount. For the 1992 simulation, the global radiation, water vapor pressure, air temperature and wind speed data were from the micrometeorological mast; for 1998 the meteorological data were from the meteorological station nearby where the micrometeorological data is not available. Crop height, leaf area index, rooting depth and density were also used and interpolated to daily scale resolution.

4.1. Reflectance

Reflectance of the wheat canopy is defined as the ratio of upward (visible and near infrared radiation) to downward solar irradiance. The measured and simulated reflectances are generally in good agreement on days of year (DOY) 104, 1992 except for sunset and sunrise (Fig. 4).

4.2. Surface energy fluxes in 1992

The comparisons of simulated and measured half-hour surface energy fluxes by Bowen ratio-energy balance method in 1992 are presented in Figs. 5

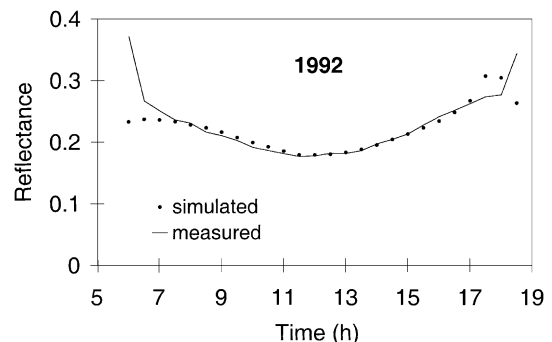


Fig. 4. Comparison of the simulated reflectance of canopy measured in 1992.

Table 1
Input parameters used in the model

Symbol	Definition model dimension	Adopted value in current	References
B	Empirical constant in Eqs. (41) and (42)	4.9	Sellers et al. (1996)
b	Empirical regression coefficient in Eq. (36)	$0.008 \text{ mol m}^{-2} \text{ s}^{-1}$	Leuning et al. (1995)
b_f	Weighting factor in Eq. (39)	0.885	Camillo et al. (1986)
C_1	Constant in Eq. (B.5)	0.95	Sellers et al. (1992)
C_2	Constant in Eq. (B.6)	0.96	Sellers et al. (1992)
C_p	Specific heat of air at constant pressure	$1010 \text{ J kg}^{-1} \text{ K}^{-1}$	Brutsaert (1988)
EXT_w	Extinction coefficient of wind	2.5	Shuttleworth and Wallace (1985)
EXT_v	Leaf nitrogen extinction coefficient in canopy in Eq. (33)	0.6	Leuning et al. (1995)
J_{\max}	Maximum potential rate of whole chain electron transport	$2.1 V_m \mu \text{ mol m}^{-2} \text{ s}^{-1}$	Su et al. (1996)
K_c	Michaelis constant for CO_2	$30 \times 2.1 Q_{10}$	Sellers et al. (1996)
k_h	Thermal molecular diffusivity	$2.42 \times 10^{-5} \text{ m}^2 \text{ s}^{-1}$	Brutsaert (1988)
K_o	Michaelis constant for O_2	$30,000 \times 1.2 Q_{10} \text{ Pa}$	Sellers et al. (1996)
$K_{w,s}$	Saturated soil water conductivity	$3.5 \times 10^{-5} \text{ m s}^{-1}$	Sellers et al. (1996)
k_s	Soil solid thermal conductivity	$0.8 \text{ W m}^{-1} \text{ K}^{-1}$	Acs (1994)
k_w	Water thermal conductivity	$0.574 \text{ W m}^{-1} \text{ K}^{-1}$	Acs (1994)
m	Empirical regression coefficient in Eq. (36)	11	Leuning et al. (1995)
O_2	Intercellular concentration of O_2	$2.09 \times 10^4 \text{ Pa}$	Sellers et al. (1992)
Q_{10}	Temperature coefficient (the relative increase of a parameter in response to 10°C temperature increase)	$(T_a - 25)/10$	Sellers et al. (1996)
S	Rubisco specificity for CO_2 relative to O_2	$2600 \times 0.57 Q_{10}$	Sellers et al. (1996)
$V_{m,0}$	Maximum catalytic capacity of rubisco at the top canopy	$200 \mu \text{ mol m}^{-2} \text{ s}^{-1}$	Sellers et al. (1996)
VPD_{SO}	Empirical coefficient in Eq. (36)	1.5 kPa	Leuning et al. (1995)
w	Characteristic dimension of an individual leaf	0.005 m	Taken according to field crop
$z_{o,g}$	Roughness length for soil surface	0.005 m	Acs (1994)
α_q	Quantum efficiency	0.385	Su et al. (1996)
ε_a	Apparent emissivity	0.98	Matsushima and Kondo (1997)
ε_c	Emissivity of canopy	0.98	Acs (1994)
ε_g	Emissivity of substrate soil	0.95	Acs (1994)
Γ^*	CO_2 compensation point	$0.5 \text{ O}_2/S \text{ Pa}$	Sellers et al. (1996)
γ	Psychrometric constant	0.645 hPa K^{-1}	
η_s	Saturated soil moisture or porosity	0.45	Measured in field
ϑ	Curvature factor	0.92	Su et al. (1996)
κ	von Karman constant	0.4	Brutsaert (1988)
λ	Latent heat of vaporization for water	$2.46 \times 10^6 \text{ J kg}^{-1}$	Brutsaert (1988)
ν	Kinematic molecular diffusivity of air	$1.51 \times 10^{-5} \text{ m}^2 \text{ s}^{-1}$	Brutsaert (1988)
ρ	Leaf reflection	0.1 for VIS; 0.4 for NIR	Norman (1985)
ρ_a	Air density	1.29 kg m^{-3}	Brutsaert (1988)
σ_1	Leaf scattering coefficient	0.2 for VIS; 0.8 for NIR	Norman (1985)
τ	Transmission	0.1 for VIS; 0.4 for NIR	Norman (1985)
ψ_{cr}	Critical soil moisture at which transpiration ceases	-150 m	Verseghy et al. (1993)
ψ_s	Saturated soil water potential	0.07 m	Sellers et al. (1996)

and 6. Fig. 5 presents the comparison from DOY 85 to DOY 88 when canopy was sparse with L being 2. Fig. 6 presents the comparison from DOY 102 to DOY 106 when canopy was closed with L being 4.5 and crop height 0.7 m. The simulated surface fluxes are in good agreement with the observations. The model can thus be applied to dense and sparse

canopies. The model underestimated net radiation at night more so in the sparse case. Maximum soil heat flux was 100 W m^{-2} and it was also underestimated at night when it is a major component of the surface energy budget. The discrepancy is larger for a sparse canopy. The simulated latent heat fluxes is slightly lower at noon. The high water VPD and irradiance at

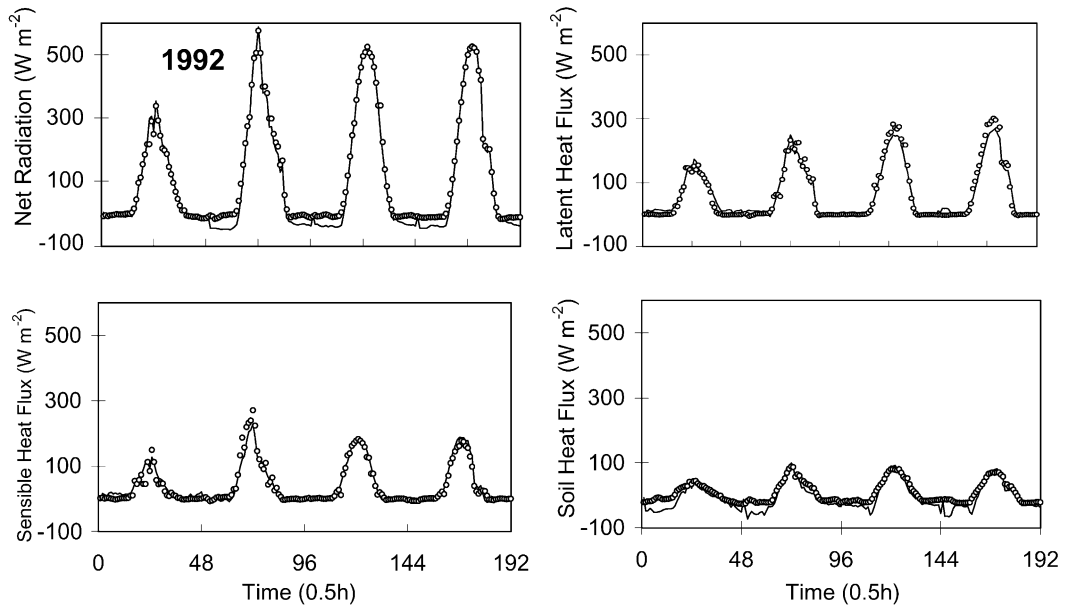


Fig. 5. Comparisons of the simulated (solid line) net radiation, latent, sensible and soil heat fluxes with the measurements (circle) of Bowen ratio-energy balance over sparse canopy in 1992.

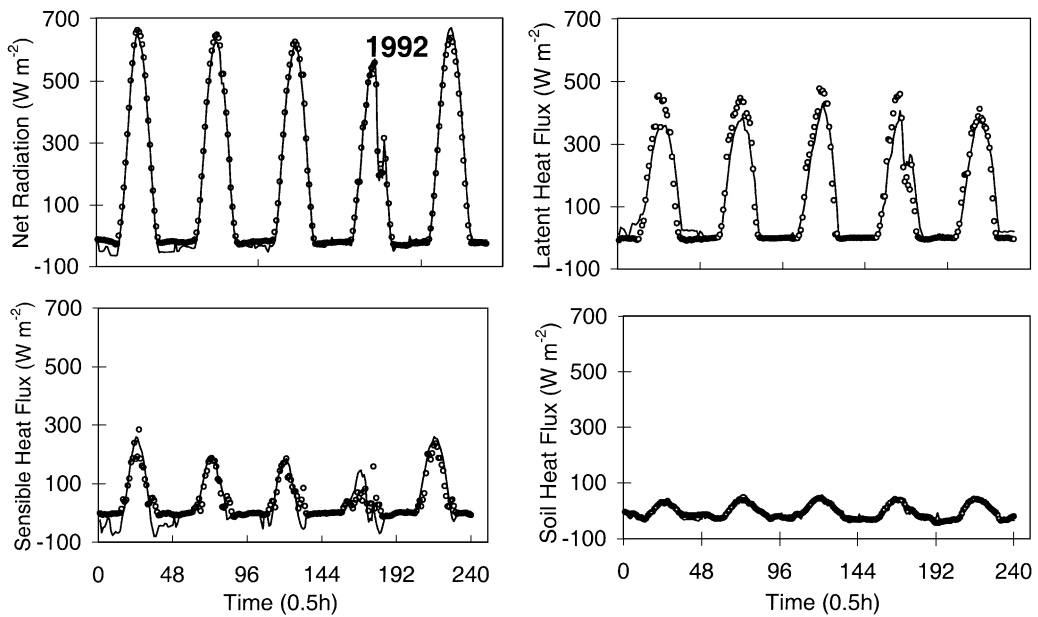


Fig. 6. The same as Fig. 5, but for dense canopy.

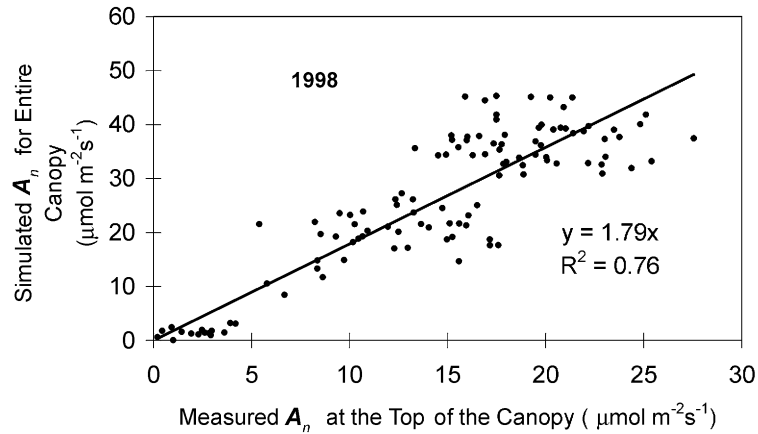


Fig. 7. Comparison of the simulated canopy assimilation rate with the measurements at the top of canopy in 1998.

noon may cause some responses of leaf stomata, but the present submodel for stomatal conductance cannot sufficiently account for this process. The situation is more obvious in the dense situation than in sparse case. The simulated sensible heat flux is sometimes negative over sunrise and sunset. The situation again is more prominent in dense crops.

4.3. Assimilation rate

Fig. 7 represents the relation of the simulated canopy assimilation rate with the measurements at the top of canopy in April and May 1998. Considering the high variability of leaf photosynthesis, the measured points are somewhat scattered, however, they are

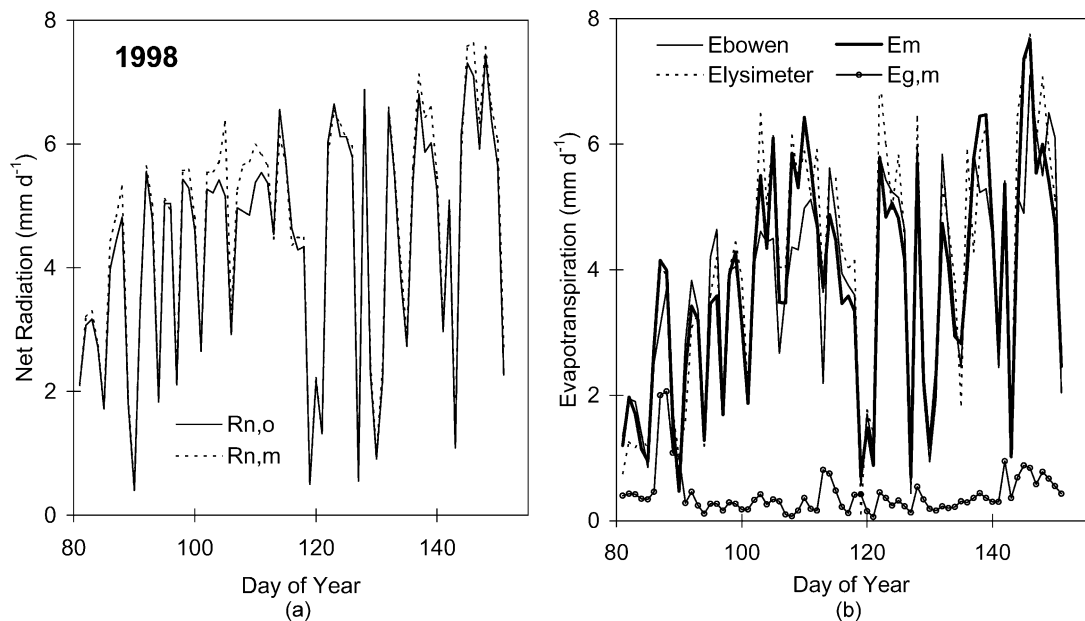


Fig. 8. Seasonal variation of net radiation (a), evapotranspiration and its components (b) from recovering green to maturity in 1998 ($R_{n,o}$: observed net radiation; $R_{n,m}$: simulated net radiation; E_{Bowen} : evapotranspiration measured by Bowen ratio method; E_M : simulated evapotranspiration; $E_{lysimeter}$: evapotranspiration measured by lysimeter, $E_{g,m}$: simulated soil evaporation).

highly correlated with a correlation coefficient being 0.87 ($R^2 = 0.76$). The best fitting slope through origin is 1.79, which indicates that the total assimilation rate is about 1.79 times of that at the canopy top.

4.4. Net radiation, evapotranspiration and soil evaporation in 1998

Net radiation above canopy, evapotranspiration and soil evaporation from recovering green to maturity stage in 1998 are shown in Fig. 8. The day-to-day variability of evapotranspiration was significant, sometimes the evapotranspiration might exceed the net radiation under situations of strong hot and dry air prevailing, such as DOY 145 and DOY 146. The soil evaporation increased rapidly after rainfall or irrigation as shown in Fig. 3. Generally speaking, the proportion of soil evaporation to total evapotranspiration was high with cloudy sky and low net radiation. Under these conditions, stomata were closed and transpiring was reduced. For sunny condition with high net radiation, canopy transpiration was the

most significant part of evapotranspiration. Under the dense canopy ($L = 4.5$, DOY 100–130), evaporation from soil surface was about 16% of total evapotranspiration. At the beginning of June (DOY 152), the winter wheat became mature and the green leaf area decreased rapidly, allowing the soil surface to absorb much more solar energy. Evaporation from wet soil surface then reached 30% of the total evapotranspiration. From the recovering to maturity stage, on average the proportion of evaporation from soil surface to evapotranspiration was about 20%.

The measured and the simulated net radiation are in good agreement with a correlation coefficient being 0.99 ($R^2 = 0.98$). The evapotranspiration measured by the Bowen ratio method and the lysimeter is in reasonable agreement with a correlation coefficient being 0.95 ($R^2 = 0.91$). Also the simulated evapotranspiration is in good agreement with the measurements via the lysimeter and the Bowen ratio method with a correlation coefficient being 0.92 ($R^2 = 0.85$) and 0.95 ($R^2 = 0.91$), respectively, as shown in Fig. 9.

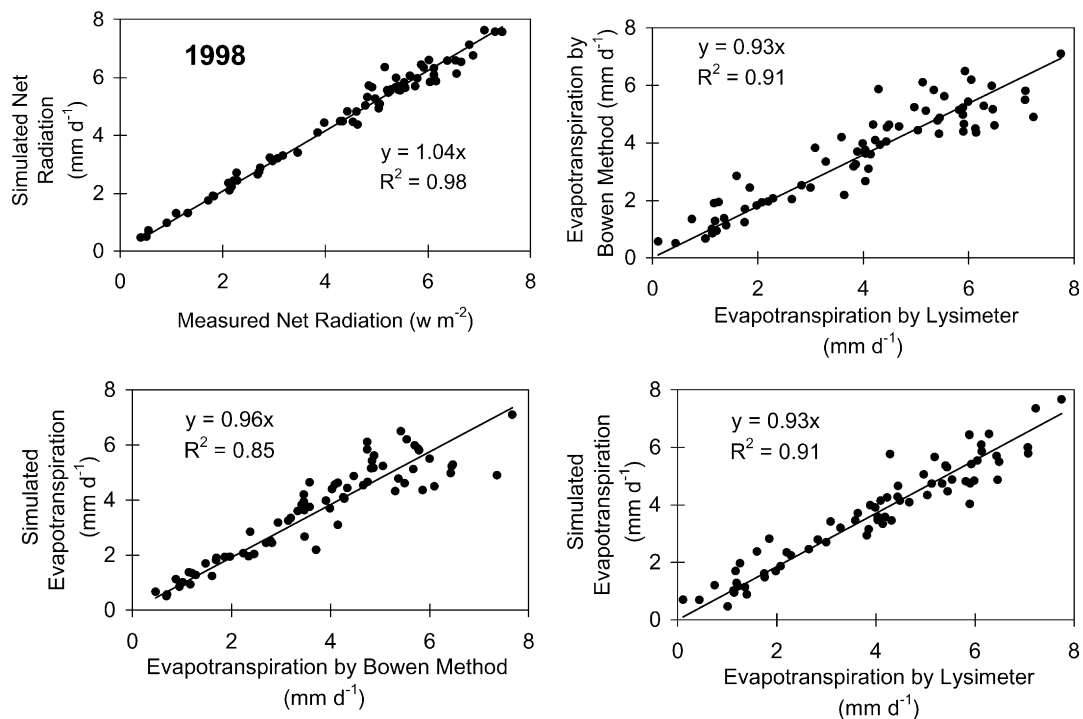


Fig. 9. Comparison of simulated and measured net radiation and evapotranspiration in 1998.

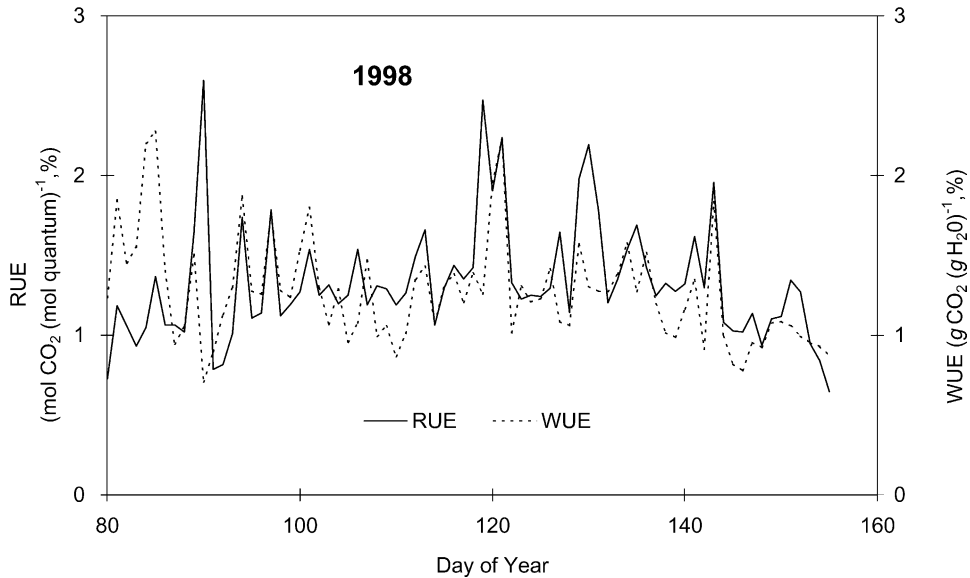


Fig. 10. Seasonal variation of net RUE and WUE from recovering green to maturity in 1998.

4.5. Radiation and water use efficiency

Fig. 10 presents the seasonal radiation and water use efficiency from March to June in 1998. The radiation use efficiency ($=A_n/\text{absorbed PAR}$, named RUE) did not change greatly in this period. In the early stage, the efficiency was a little lower. The water use efficiency ($=A_n/\text{evapotranspiration}$, named WUE) was high in March (DOY 80–90) with the maximum of 2.5%, then decreased slightly in April and May to a maximum of 1.5%. This was probably due to canopy capturing less incident radiation in the early stage, whereas the relative fraction of sunlit leaf was high. Thus RUE was lower but WUE was higher than the following period with high leaf area index. RUE and WUE all correlated negatively with net radiation and evapotranspiration (Fig. 8). For the entire period, WUE and RUE were both about 1.2% on average.

4.6. Surface temperature

The surface temperature is a key parameter for surface turbulent fluxes and aerodynamic resistance. With the expanding availability of remotely sensed data, radiometric surface temperature is often used as either input or as a validation of SVAT models. A compari-

son of radiometric surface temperature with the simulated surface temperature is shown in Fig. 11 for the 1992 and 1998 growing seasons. The respective correlation coefficients are 0.96 ($R^2 = 0.93$) and 0.97 ($R^2 = 0.94$) and the best fitting slopes through the origin are 1.01 and 1.02. The root mean square differences between the simulated and the radiometric surface temperature are 1.4 and 1.3°C in 1992 and 1998, respectively. This result confirmed that the model output is acceptable for turbulent fluxes. The good agreement between the radiometric and simulated surface temperatures identifies that the parameterization in the model is effective.

4.7. Soil moisture

Depletion of soil moisture is caused by root extraction and soil evaporation. For our winter wheat, the root is mainly located in the upper 0.2–0.3 m. There is usually a plough pan of clay under this depth. The comparison of soil moisture between the simulated and the observation in 1998 is shown in Fig. 12, from which irrigation or heavy rainfall (Fig. 3) increased soil moisture to field capacity and made peaks of soil moisture variation. The drying period after peaks was about 25 days. The simulated soil moisture of 0–0.2 m

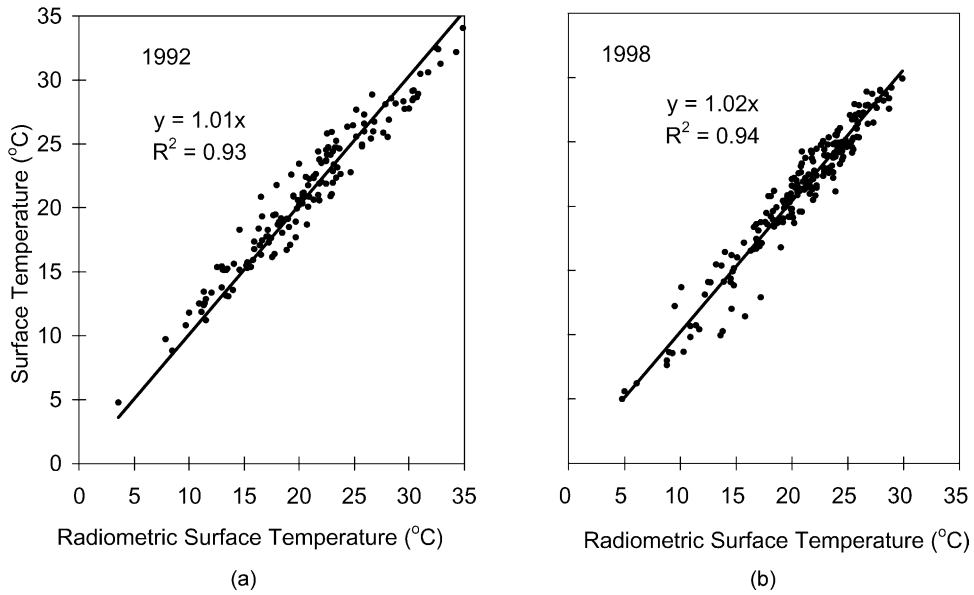


Fig. 11. Comparison of the radiometric surface temperature with the simulated surface temperature: (a) in 1992; (b) in 1998.

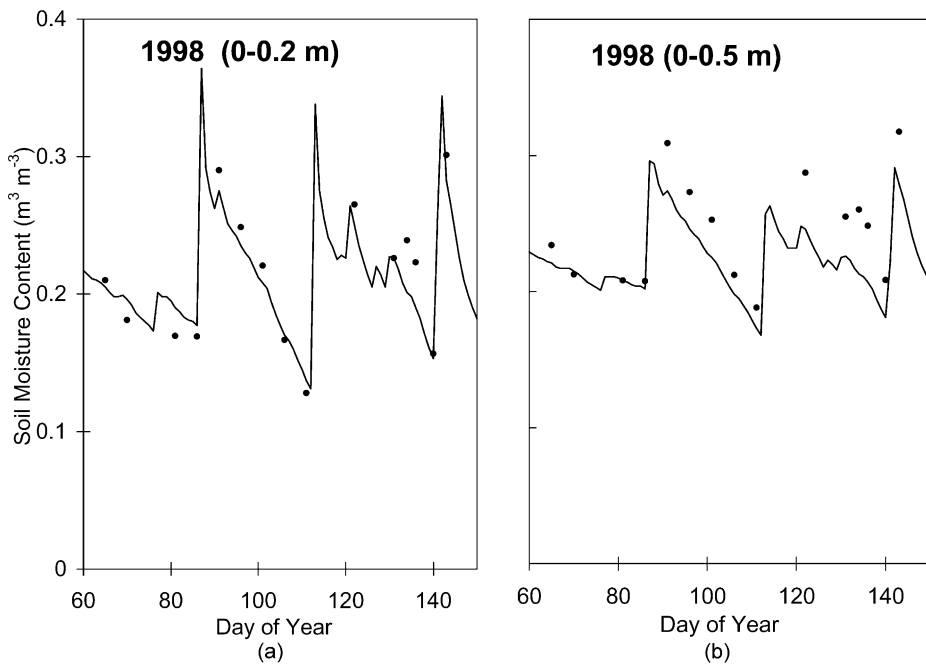


Fig. 12. Comparison of simulated soil moisture (solid line) with the measurements (circle) in 1998: (a) 0–0.2 m; (b) 0–0.5 m.

layer is in quite good agreement with the measurements, however, the 0–0.5 m layer is not as good. The reason is that in the 0–0.2 m layer soil moisture is affected markedly by evapotranspiration, but under plough pan the upward movement of soil moisture is hindered somewhat, and a homogeneous profile assumption cannot describe these effects well enough.

5. Sensitivity analysis

5.1. Different stomatal conductance schemes

The nature of the canopy stomatal model is central to simulate canopy transpiration and available energy partitioning into latent and sensible heat. Three models are discussed here, namely, the Jarvis model (Acs, 1994), the Ball–Berry model (Sellers et al., 1996) and the Leuning model (Leuning et al., 1995). The Jarvis model treats the stomatal conductance as an entity that is independent of both photosynthesis and transpiration, and is constructed as a product of several independent functions of environmental factors. However, the Ball–Berry and Leuning models link intimately the stomatal conductance and photosynthesis and thus require fewer parameters. The difference of the Ball–Berry and Leuning models is that the Ball–Berry scheme relates the net photosynthesis with

relative humidity at the leaf surface, whereas the Leuning model uses water VPD instead.

Seasonal evapotranspiration in 1998 simulated from the three models is presented in Fig. 13. Overall, the results are similar to each other, but significant differences appear when the water VPD is high, corresponding to the peaks shown in Fig. 13. The Jarvis model respond to VPD much more sensitively than the Leuning model. The Ball–Berry model was not so sensitive to VPD. By analyzing the correlation between measured evapotranspiration (measured by the lysimeter) and simulated evapotranspiration, it is found that the Leuning model gives the highest correlation coefficient being 0.95, then the Ball–Berry model (0.93), the Jarvis model (0.91). The Leuning model's result is therefore slightly better than the other two by this measure.

5.2. Scaling up from leaf to canopy

We discuss two kinds of scaling up methods, namely sunlit/shaded leaves and traditional big leaf schemes. Canopy assimilate rates in 1998 calculated by these two schemes are shown in Fig. 14. For dense canopy and sunny days, the relative difference between the traditional big leaf scheme and sunlit/shaded scheme is more than 40%, but for low leaf area index and cloudy days (before DOY 80), the difference is much

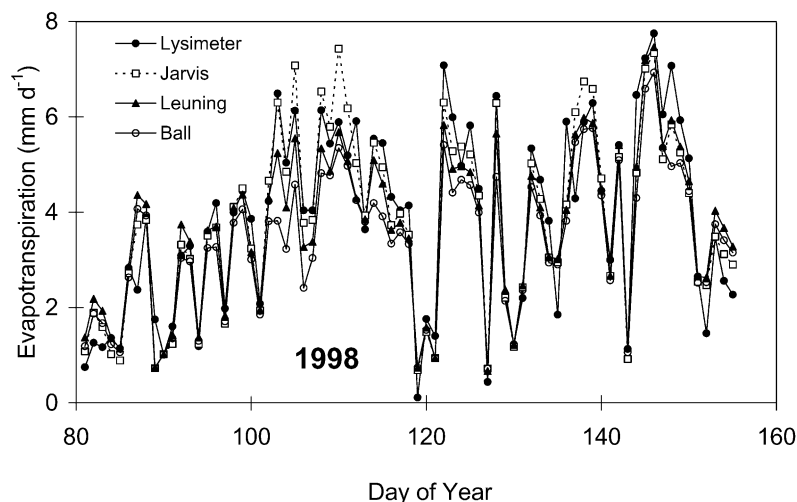


Fig. 13. Comparisons of seasonal evapotranspiration simulated with the Jarvis, Ball–Berry and Leuning stomatal conductance model, respectively.

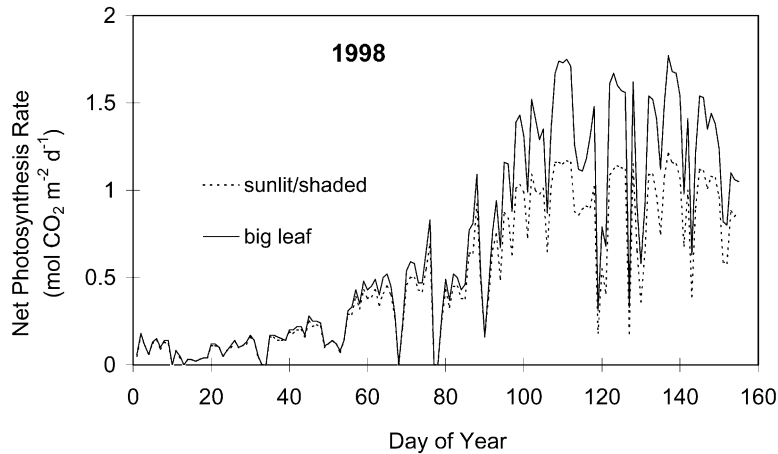


Fig. 14. Comparison of net photosynthesis rate simulated with sunlit/shaded and one big leaf scheme.

less. The distinction of sunlit and shaded leaves is not important when most of the incident irradiance is diffuse during cloudy days. However the situation is quite different for sunny days. On the other hand, if the canopy is sparse with a high fraction of sunlit leaves, this reduces the bias of traditional big leaf scheme. On average, the relative difference between the two is about 33%. For total evapotranspiration, it is only 5% (not shown in this paper). Although the difference for evaporation is minor compared with an evapotranspiration measurement error of 20%, the difference for canopy assimilation rate is evident. In this aspect, the distinction is especially meaningful for canopy assimilation simulation.

6. Conclusions

Satisfactory agreement was obtained between simulations and measurements for energy fluxes, surface temperature, soil moisture and canopy net photosynthesis rate. Daily evapotranspiration rates are in good agreement with measurements taken by both lysimeter and Bowen ratio-energy balance methods. The simulated assimilation rates for the whole of the canopy layer correlated well with the rates measured at the top layer of the canopy. The simulated canopy-scale assimilation rate was 1.8 times that measured at the leaf scale near the top of the canopy. It would be desirable to further test the model by using eddy cor-

relation measurement of CO₂ flux above a crop. The model could be extended to estimating net ecosystem productivity by incorporating a complete respiration (plant and soil) component, currently under development.

Model predicted soil moisture in the top 0.2 m is in good agreement with the measurements, but the top 0.5 m soil moisture total is somewhat underestimated. Sensitivity results show that the Leuning type scheme may give slightly better evapotranspiration results. There is not a great deal of difference between evapotranspiration calculated from the present model and “single leaf” model. However, the two models differ considerably in their respective photosynthesis estimates. This emphasizes the need to parameterize for sunlit and shaded leaves when constructing photosynthesis models.

The input variables required in our model can be standard climatological station data, as shown in 1998 application. This opens the way for general practical application of the model beyond the restrictions of data derived from micrometeorological instrumentation.

Acknowledgements

We are greatly indebted to the Chinese National Natural Science Foundation (Project No. 49771019, 49890330) and Institute of Geographical Sciences and Natural Resources Research (Innovation Knowledge

Project No. CXIOG-C00-05-01) for funding this research. Many thanks to Yucheng and Datun Experimental Stations, Institute of Geography, Chinese Academy of Sciences for kindly providing data in 1998 via Prof. Xianqun Xie and Dr. Qiang Yu and for cooperatively collecting data in 1992 in association with Profs. Yueqin Xiang and Xiaomin Sun. We very much thank two anonymous reviewers for helpful comment to the manuscripts. Many thanks to Dr. F. Kelliher (Manaaki Whenua, Landcare Research, New Zealand) and Dr. E. Bardsley (University of Waikato, New Zealand) for suggestions in improving the final manuscript.

Appendix A

A.1. Scattering of direct beam

The radiative power intercepted by a leaf is absorbed, reflected and transmitted. The fractions of upwelling and downwelling scattering components described by two-stream approximation are given as (De Ridder, 1997):

$$\alpha = \frac{1}{\pi} \int_0^{2\pi} \int_0^{\pi/2} H(\cos \Phi) \cos \theta \, d\Omega \quad (\text{A.1})$$

where $H(\cos \Phi)$ is the Heaviside step function, Φ the angle between the leaf normal vector and the radiant beam, Ω the solid angle, $d\Omega = \sin \theta \, d\theta \, d\varphi$, φ the azimuth angle, θ is defined as the same as in Eq. (2) in the text. By integrating Eq. (A.1), we have, for upper leaf surface,

$$\alpha_u^\uparrow = \frac{1}{2}(1 + \cos \theta_1) \quad (\text{A.2})$$

$$\alpha_u^\downarrow = 1 - \alpha_u^\uparrow = \frac{1}{2}(1 - \cos \theta_1) \quad (\text{A.3})$$

where θ_1 is the zenith angle of the normal vector to the leaf surface.

Similarly, for the lower leaf surface,

$$\alpha_l^\uparrow = \frac{1}{2}(1 - \cos \theta_1) \quad (\text{A.4})$$

$$\alpha_l^\downarrow = \frac{1}{2}(1 + \cos \theta_1) \quad (\text{A.5})$$

By combining leaf reflection ρ and transmission τ , the intercepted direct radiation power sent upward and downward could be calculated. In a single layer of

thickness ΔL , the upward and downward scattering coefficient is given, respectively, as,

$$\sigma_{b,u} = \frac{1}{2}[(\rho + \tau)\text{EXT}_r + (\rho - \tau)\langle \cos^2 \theta_1 \rangle] \quad (\text{A.6})$$

$$\sigma_{b,d} = \frac{1}{2}[(\rho + \tau)\text{EXT}_r - (\rho - \tau)\langle \cos^2 \theta_1 \rangle] \quad (\text{A.7})$$

EXT_r is the same as in the text, $\langle \cos^2 \theta_1 \rangle$ is defined as

$$\langle \cos^2 \theta_1 \rangle = \frac{1}{2\pi} \int_0^{2\pi} \int_0^{\pi/2} \cos^2 \theta_1 g(\theta_1) \, d\Omega_1 \quad (\text{A.8})$$

where $g(\theta_1)$ is the leaf angle distribution function. $d\Omega_1 = \sin \theta_1 \, d\theta_1 \, d\varphi_1$, φ_1 is the azimuth angle of the normal vector to the leaf surface.

A.2. Scattering of diffuse radiation

It is assumed that upward and downward diffuse radiation is isotropic. The downward flux can be decomposed into infinitesimal directional fluxes. By integrating these fluxes over the upper hemisphere, one can get the scattering coefficient for diffuse radiation upward and downward,

$$\sigma_{d,u} = \frac{1}{2}[(\rho + \tau) + (\rho - \tau)\langle \cos^2 \theta_1 \rangle] \quad (\text{A.9})$$

$$\sigma_{d,d} = \frac{1}{2}[(\rho + \tau) - (\rho - \tau)\langle \cos^2 \theta_1 \rangle] \quad (\text{A.10})$$

Appendix B

The **Ribulose-bisphosphate carboxylase-oxygenase** enzyme (Rubisco) limiting rate A_R is expressed as

$$A_R = V_m \left[\frac{c_i - \Gamma^*}{c_i + K_c(1 + O_2/K_o)} \right] \quad (\text{B.1})$$

where V_m is the maximum catalytic capacity of Rubisco ($\mu\text{mol m}^{-2} \text{s}^{-1}$), c_i , O_2 are intercellular concentration of CO_2 and O_2 (Pa), respectively, Γ^* is the CO_2 compensation point (Pa, $= 0.5 O_2/S$, S is the Rubisco specificity for CO_2 relative to O_2); K_c , K_o are Michaelis constants for CO_2 and O_2 , respectively (Pa). Terms V_m , S , K_c , K_o are all functions of temperature (see appendix of Sellers et al., 1996).

The light-limited rate of assimilation A_E is expressed as,

$$A_E = J \frac{c_i - \Gamma^*}{4.5c_i + 10.5\Gamma^*} \quad (\text{B.2})$$

where J is the potential rate of whole chain electron transport. The smaller root of the following nonrectangular hyperbola equation is chosen as the solution of J (Farquhar and Wong, 1984):

$$\vartheta J^2 - (\alpha_q Q + J_{\max})J + \alpha_q Q J_{\max} = 0 \quad (\text{B.3})$$

where J_{\max} is the maximum rate of whole chain electron transport at saturated light, taken as $2.1V_m$; Q is the absorbed PAR photon flux density ($\mu\text{mol m}^{-2} \text{s}^{-1}$). α_q is the quantum efficiency. ϑ is the curvature factor, determining the shape of the nonrectangular hyperbola.

The third limiting rate is capacity for the export or utilization of the products of photosynthesis, given as

$$A_S = \frac{1}{2} V_m \quad (\text{B.4})$$

To keep the smooth transition from one limiting rate to another, photosynthesis rate A may be determined by two quadratic equations which are solved for their smaller roots (Collatz et al., 1991),

$$C_1 A_P^2 - A_P(A_R + A_E) + A_R A_E = 0 \quad (\text{B.5})$$

$$C_2 A^2 - A(A_P + A_S) + A_P A_S = 0 \quad (\text{B.6})$$

where C_1 and C_2 are constants, A_P is the smoothed minimum of A_E and A_R .

References

- Acs, F., 1994. A coupled soil–vegetation scheme: description, parameters, validation, and sensitivity studies. *J. Appl. Meteorol.* 33, 268–284.
- Amthor, J.S., 1994. Scaling CO_2 –photosynthesis relationships from the leaf to the canopy. *Photosynth. Res.* 39, 321–350.
- Ball, J.T., Woodrow, I.E., Berry, J.A., 1987. A model predicting stomatal conductance and its contribution to the control of photosynthesis under different environmental conditions. In: Biggens, J. (Ed.), *Progress in Photosynthesis Research*, Vol. IV. Martinus Nijhoff, Dordrecht, pp. 221–224.
- Boegh, E., Soegaard, H., Friberg, T., Levy, P.E., 1999. Models of CO_2 and water vapor fluxes from a sparse millet crop in the Sahel. *Agric. For. Meteorol.* 93, 7–26.
- Brutsaert, W.H., 1988. In: *Evaporation into the Atmosphere*. Reidel, Dordrecht.
- Camillo, P.J., Gurney, R.J., 1986. A resistance parameter for bare soil evaporation models. *Soil Sci.* 141, 95–105.
- Choudhury, B.J., Monteith, J.L., 1988. A four-layer model for the heat budget of homogeneous land surfaces. *Q. J. Roy. Meteorol. Soc.* 144, 373–398.
- Choudhury, B.J., Reginato, R.J., Idso, S.B., 1986. An analysis of infrared temperature observations over wheat and calculation of latent heat flux. *Agric. For. Meteorol.* 37, 75–88.
- Clapp, R.B., Hornberger, G.M., 1978. Empirical equations for some soil hydraulic properties. *Water Resour. Res.* 14, 601–604.
- Collatz, G.J., Ball, J.T., Grivet, C., Berry, J.A., 1991. Physiological and environmental regulation of stomatal conductance, photosynthesis and transpiration: a model that includes a laminar boundary layer. *Agric. For. Meteorol.* 54, 107–136.
- De Ridder, K., 1997. Radiative transfer in the IAGL land surface model. *J. Appl. Meteorol.* 36, 12–21.
- Farquhar, G.D., Wong, S.C., 1984. An empirical model of stomatal conductance. *Aust. J. Plant Physiol.* 11, 191–210.
- Farquhar, G.D., Von, C.C., Berry, J.A., 1980. A biochemical model of photosynthetic CO_2 assimilation in leaves of C_3 species. *Planta* 149, 78–99.
- Flerchinger, G.N., Kustas, W.P., Wertz, M.A., 1998. Simulating surface energy fluxes and radiometric surface temperatures for two arid vegetation communities using the SHAW model. *J. Appl. Meteorol.* 37, 449–460.
- Goudriaan, J., 1977. *Crop micrometeorology: a simulation study*. Wageningen Center for Agricultural Publishing and Documentation, Wageningen.
- Kondo, J., 1993. Time variation in soil water content of the surface soil layer after a rainfall. *J. Jpn. Soc. Hydrol. Water Resour.* 6, 336–343 (in Japanese).
- Kondo, J., Xu, J., 1997. Seasonal variations in the heat and water balances for non-vegetated surfaces. *J. Appl. Meteorol.* 36, 1676–1695.
- Leuning, R., Kelliher, F.M., De Pury, D.G., Schulze, E.D., 1995. Leaf nitrogen, photosynthesis, conductance and transpiration: scaling from leaves to canopies. *Plant Cell Environ.* 18, 1183–1200.
- Matsushima, D., Kondo, J., 1997. A proper method for estimating sensible heat flux above a horizontal-homogeneous vegetation canopy using radiometric surface observations. *J. Appl. Meteorol.* 36, 1696–1711.
- Mihailovic, D.T., Ruml, R., 1996. Design of land–air parameterization scheme (LAPS) for modeling boundary layer surface processes. *Meteorol. Atmos. Phys.* 58, 65–81.
- Myneni, R.B., Ganapol, B.D., 1992. Remote sensing of vegetation canopy photosynthetic and stomatal conductance efficiencies. *Remote Sens. Environ.* 42, 217–238.
- Norman, J., 1985. Modeling the complete crop canopy. In: Baarfield, B., Gerber, J. (Eds.), *Modification of the Aerial Environment of Crops*. Am. Soc. Agric. Eng. Monograph No. 2, ASAE, St. Joseph, Michigan, pp. 249–277.
- Pielke, R.A., 1984. In: *Mesoscale Meteorological Modeling*. Academic Press, New York, 612 pp.
- Sellers, P.J., Berry, J.A., Collatz, G.J., Field, C.B., Hall, F.G., 1992. Canopy reflectance, photosynthesis and transpiration. Part III: A re-analysis using improved leaf models and a new canopy integration scheme. *Remote Sens. Environ.* 42, 187–216.
- Sellers, P.J., Randall, D.A., Collatz, G.J., Berry, T.A., Field, C.B., 1996. A revised land surface parameterization (SIB2) for

- atmospheric GCMs. Part I: Model formulation. *J. Climate* 9, 676–705.
- Shaw, R.H., Pereira, A.R., 1982. Aerodynamic roughness of a plant canopy: a numerical experiment. *Agric. Meteorol.* 26, 51–65.
- Shuttleworth, W.J., Wallace, J.S., 1985. Evaporation from sparse crops—an energy combination theory. *Q. J. Roy. Meteorol. Soc.* 111, 839–855.
- Su, H., Paw, U.K., Shaw, R.H., 1996. Development of a coupled leaf and canopy model for the simulation of plant–atmosphere interaction. *J. Appl. Meteorol.* 35, 733–750.
- Tourula, T., Heikiheimo, M., 1998. Modeling evapotranspiration from a barley field over the growing season. *Agric. For. Meteorol.* 91, 237–250.
- Verseghy, D.L., McFarlane, N.A., Lazare, M., 1993. CLASS — A Canadian land surface scheme for GCMs. II. Vegetation model and coupled runs. *Int. J. Climatol.* 13, 347–370.
- Wang, Y., Leuning, R., 1998. A two-leaf model for canopy conductance, photosynthesis and partitioning of available energy. I. Model description and comparison with a multi-layered model. *Agric. For. Meteorol.* 91, 89–111.
- Watanabe, T., Mizutani, K., 1996. Model study on micro-meteorological aspects of rainfall interception over an evergreen broad-leaved forest. *Agric. For. Meteorol.* 80, 195–214.
- Zuo, D., Zhou, Y., Xiang, Y., Zhu, Z., Xie, X., 1991. *Studies on Radiation in the Epigeosphere*. Academic Press, Beijing, 469 pp. (in Chinese).